THE ASTROPHYSICAL JOURNAL, 449:681–687, 1995 August 20

A *ROSAT*-DETECTED, NEW GALACTIC SUPERNOVA REMNANT IN SAGITTARIUS, G13.3−1.3

F. D. SEWARD AND T. M. DAME
Harvard-Smithsonian Center for Astrophysics, 60 Garden Street, Cambridge, MA 02138
R. A. FESEN
Dartmouth College, Department of Physics and Astronomy, 6127 Wilder Laboratory, Hanover, NH 03755
AND
B. ASCHENBACH
Max-Planck-Institut fur Extraterrestrische Physik, Giessenbachstrasse, D-85740 Garching, Germany
Received 1994 December 16; accepted 1995 March 2

ABSTRACT

Faint and diffuse soft X-ray emission, coincident with [S II] strong optical filaments, probably marks a previously unrecognized supernova remnant (SNR) in Sagittarius ($l = 13.3$, $b = -1.3$). *ROSAT* PSPC data show soft X-rays from an area $40' \times 70'$ with a flux of 1.3×10^{-11} erg cm^{-2} s^{-1} between 0.1–2.4 keV. Optical interference-filter images taken of the region reveal a 20′ long complex of relatively bright filaments located along the south central boundary of the X-ray region which may be associated with a ridge of faint 11 cm continuum emission. Optical spectra of these filaments show strong [S II] $\lambda\lambda$6716, 6731 emission ([S II]/Hα = 0.85) and [O I] $\lambda\lambda$6300, 6364 characteristic of shocked interstellar gas found in SNRs. Both X-rays and optical emissions along the source's NE extent show strong absorption by the dust regions Lynds 332, 336, and 342, indicating a location behind these nebulae. CO emission from this region has been mapped and a kinematic distance derived for absorbing material. The remnant is shown to lie between two absorbing regions located at distances of 2 and 4 kpc.

Subject headings: ISM: individual (G13.3−1.3) — supernova remnants — X-rays: ISM

1. INTRODUCTION

The detection of new Galactic supernova remnants (SNRs) has been generally accomplished through deep radio surveys for nonthermal emission in the Galactic plane (Green 1991). New searches continue to identify new Galactic SNRs and it has been suggested that several hundred Galactic SNRs detectable with current instruments await identification (Helfand et al. 1989). During the *ROSAT* All-Sky Survey (Aschenbach 1993), several diffuse X-ray sources were found near the Galactic plane with one of these identified as a previously unrecognized SNR (Pfeffermann, Aschenbach, & Predehl 1991). This object, RX J0459.1+5147 (G156.2+5.7) appears as a circular, limb-brightened region, 1°.8 in diameter. Subsequent radio observations have confirmed it as a SNR (Reich, Fürst, & Arnal 1992) with a radio surface brightness about four times fainter than any other Galactic SNR.

This unexpected discovery of an X-ray bright, yet radio faint SNR raises the possibility of finding other X-ray-emitting Galactic SNRs which might have been missed in radio surveys or missed because of bright neighboring sources (e.g., the SNR CTB 109 near Cas A; Gregory & Fahlman 1980; Hughes, Harten, & van den Bergh 1981). In order to investigate this possibility, the spatial structure of several weak extended sources serendipiously discovered in the *ROSAT* All-Sky survey has been investigated with pointed *ROSAT* observations. In this paper, we describe the results for one of these sources RX J1819.5−1800, located near the Galactic plane in Sagittarius, which appears to be a new probable SNR.

2. OBSERVATIONS

2.1. *X-ray Morphology and Spectrum*

The *ROSAT* telescope with the Position Sensitive Proportional Counter (PSPC) at the focus was pointed at $\alpha[2000] = 18^h19^m14^s.3$, $\delta[2000] = -18°09'36''$ during 1993 September 13 and 15. A total of 5991 seconds of data were received after standard processing. The count rate versus time was inspected to search for times of increased background due to scattered solar X-rays or charged particles. No anomalies were found, and the entire 5991 seconds were used in the analysis. There are no bright unresolved sources in the field and diffuse emission from the SNR is faint.

Figure 1 shows diffuse X-ray emission as it appears in the 2° diameter PSPC field. Data have been restricted to pulse heights between 0.4 and 1.8 keV. The "background" outside the remnant is not uniform in that the emission west of the remnant is brighter than that in the south and east.

Table 1 lists five unresolved sources which lie in the direction of RX J1819.5−1800. Four of these are indicated in Figure 2 by arrows. Three are obvious in the raw data. The brightest (southeast) source is associated with the sixth magnitude O8 star HD 167771. A weaker, nearby source elongates this image and might be due to the 10th magnitude B5 star HD 313036. However, there are other B5 stars of this magnitude in the field that are not detected as X-ray sources. A seventh-magnitude B0 star, HD 168021, coincides with the second brightest (south) source. An X-ray source, with no obvious optical counterpart, lies close to the center of the diffuse emission as defined by the ellipse shown in Figure 2. Another source is just inside the SE rim. Only the O8 star shows clearly in Figure 1 because the data have been smoothed to enhance visibility of the diffuse emission.

There are two radio pulsars in the *ROSAT* field (Taylor, Manchester, & Lyne 1993). The pulsar PSR J1820−1818 ($P = 0.31$ s, $\tau = 5 \times 10^7$ years) lies close to the SE boundary of RX J1819.5−1800 but is not detected. The pulsar J1816−17 ($P = 0.78$ s, $\tau = 1.7 \times 10^6$ years) is at the top edge of the *ROSAT* field and is also not detected. Since both pulsars are

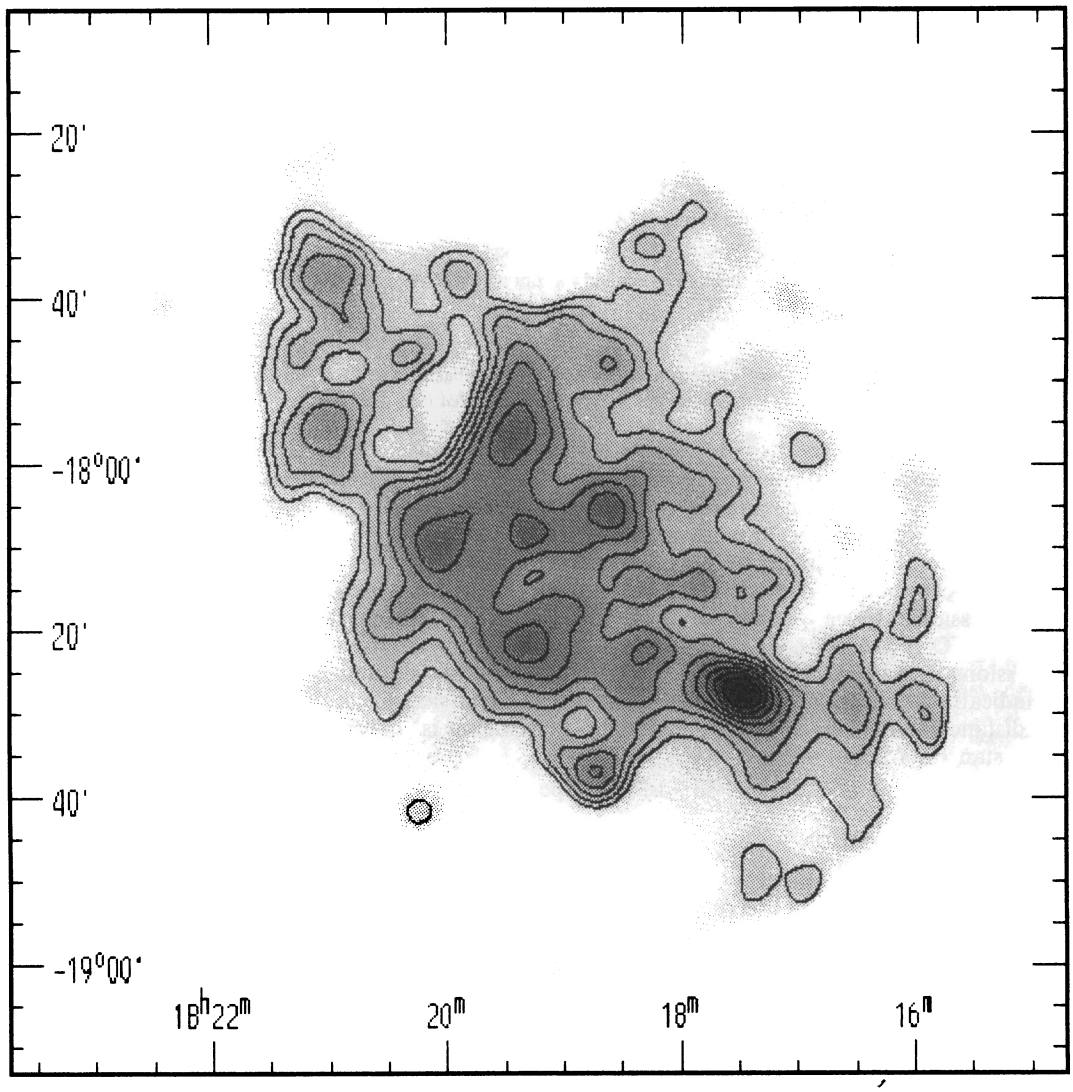

FIG. 1.—*ROSAT* picture of G13.3−1.3 (RX J1819.5−1800). Data have been smoothed with a Gaussian function with FWHM of 4'.7. Contours of constant surface brightness are overlaid on the gray-scale picture. The remnant is faint. Contours are logarithmic and spaced a factor of only 1.11. The central features are a factor of 1.8 brighter than the outer contour. The bright unresolved source at the southwestern edge is an O star.

old and the electron-dispersion distance for both is over 6 kpc, we assume neither is associated with the SNR.

The X-ray emission structure is complex and it is difficult to ascertain the true western edge of the diffuse emission. X-rays appear to come from an elliptically shaped area $\sim 40' \times 70'$ in extent with the long axis oriented NE-SW. The two unresolved sources close to the southwest boundary (see arrows in Fig. 2) make the remnant seem to extend further in this direction. The X-ray source's southern extent is consistent with the location of the optical filaments. Emission is strongest from a central region $\sim 30'$ in diameter. Emission northeast of this area is definite, but weaker. A distinct line of absorption runs north-to-south through the northeast quadrant and separates the northeast and central parts. The optical data indicate that this feature is due to absorption. Because the X-ray emission is weak here, this cannot be investigated using the X-ray spectrum. However this feature does not line up with the window-support rib and appears to be a real feature of the diffuse

TABLE 1

UNRESOLVED SOURCES

R.A. (2000)	Declination (2000)	Count Rate (counts ks^{-1})	Remarks
$18^h17^m16^s.6$.....	−18°28'21"	18.7	HD 313036?, 10, B5
18 17 29.5.....	−18 27 56	25.5	HD 167771, 6.6, O8
18 18 47.1.....	−18 37 08	14.0	HD 168021, 7.1, B0IB
18 19 24.9.....	−18 09 12	5.0 ± 1.0	Close to center of remnant
18 20 4.0.....	−18 12 05	5.1 ± 1.0	Close to SE limb

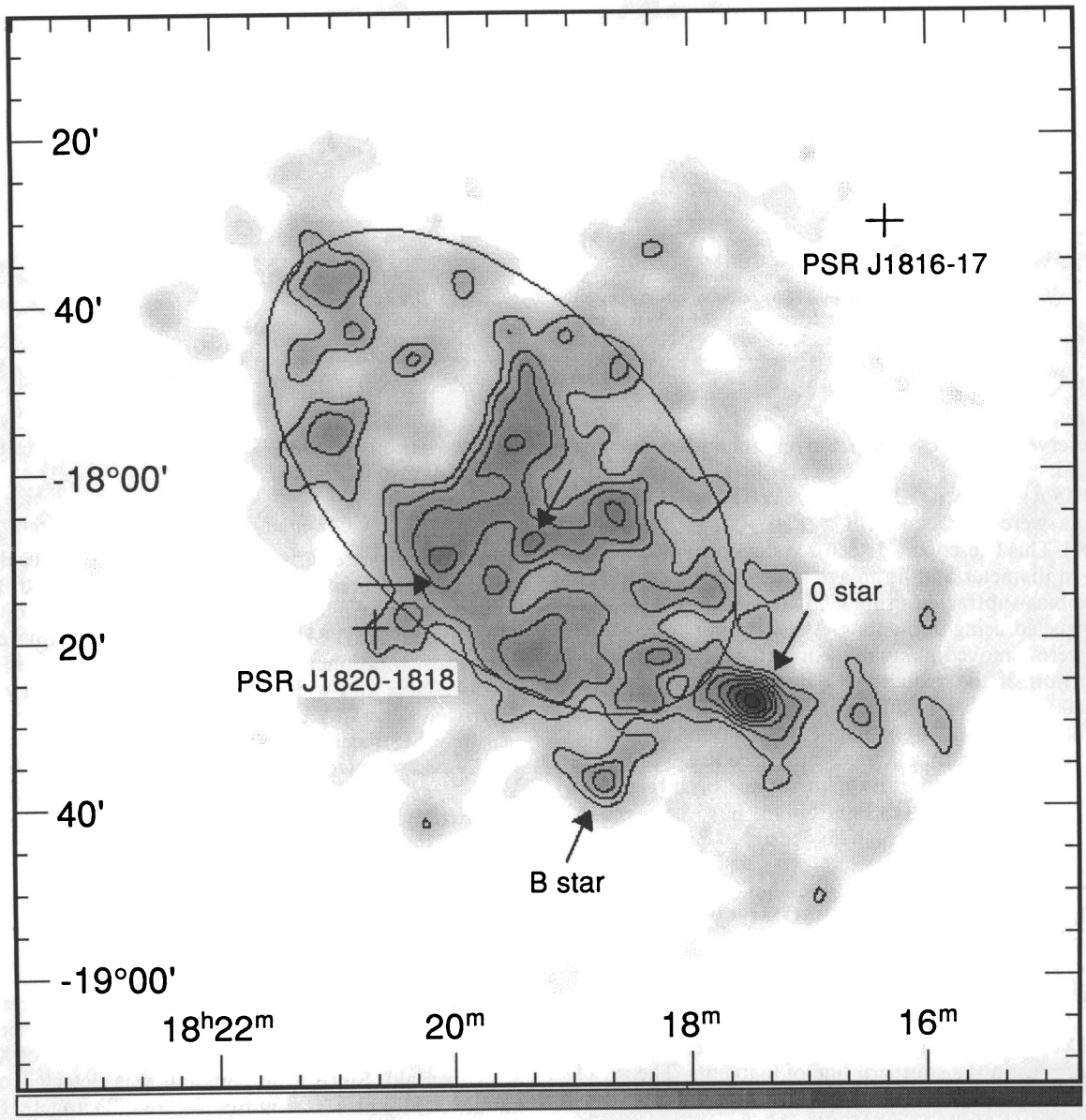

FIG. 2.—*ROSAT* data smoothed with a Gaussian function with FWHM of 3.5. Contours showing the brighter regions are overlaid on a gray-scale picture. The ellipse illustrates the approximate extent of the remnant. Note the variable "background" outside the remnant. Positions of unresolved X-ray sources are indicated by arrows and those of radio pulsars by crosses.

emission. X-ray properties of RX J1819.5 – 1800 are listed in Table 2.

The uncertainty in the count rate is due to uncertainty in background subtraction. An average between emission east and west of RX J1819.5 – 1800 has been used for background. The X-ray spectrum of the central region was analyzed using IRAF PROS and XSPEC software. The spectrum is clearly absorbed. No photons below 0.4 keV were detected above background and at least $\approx 10^{21}$ atoms cm^{-2} of interstellar material is needed in the line of sight. Although a single-temperature Raymond model can produce a fit to the observation with reduced $\chi^2 \leq 1$, there is always a slight excess of high- and low-energy photons. A two-temperature model gives a better fit (again with reduced $\chi^2 \leq 1$). Given any absorption between 10^{21} and 10^{22} atoms cm^{-2}, a combination of reasonable temperatures can be found which fit the data; not surprising because the energy span of these data is not large enough to determine an accurate temperature. Because the optical filament spectra indicate a low column density, we assume a low column density to characterize the X-ray emission. A set of parameters which fit the optical-measured column is listed in Table 2.

2.2. *Associated Optical Emission*

The Palomar Observatory Sky Survey (POSS) shows that the X-ray source is coincident with a diffuse H II region, LBN 52 (Lynds 1965). This emission is in a dense star field area surrounded by several prominent dust lanes. Despite a lack of filamentary emission readily apparent in the POSS prints, a search for optical filaments associated with the *ROSAT* diffuse

TABLE 2

X-RAY PROPERTIES OF G13.3−1.3

Parameter	Value
Center (epoch 2000)	$18^h19^m34^s$ −18°00′
Size	40′ × 70′
Count rate (counts s^{-1})	1.5 ± 0.4
Spectrum	Thermal (assumed)
Two-temperature Fit	
Temperature (not unique)	67% (0.3 keV), 33% (1.0 keV)
Absorption (not unique) (atoms cm^{-2})	1.0×10^{21}
Flux at detector (0.1–2.4 keV) (erg cm^{-2} s^{-1})	1.3×10^{-11}
L_X (0.1–2.4 keV) (ergs s^{-1})	3×10^{34} (at 3.3 kpc)

X-ray source was undertaken in 1993 August using the Case Western Reserve University 0.6 m Burrell Schmidt Telescope at Kitt Peak. Single 10 minute exposures through Hα (FWHM = 15 Å) and [S II] 6716, 6731 (FWHM = 80 Å) interference filters were obtained with a 2048 × 2048 Tektronix CCD (S2KA). This telescope + detector system provided a field of view 69′ in diameter and an image scale 2.″03 $pixel^{-1}$. The images were bias-subtracted using CCD overscan regions and flat-field corrected using dome flats. A few prominent cosmic-ray "hits" were removed manually using IRAF software routines. A portion of the reduced Hα image centered on RX J1819.5−1800 is shown in Figure 3 (Plate 20). This image shows a 20′ long line of sharp filaments positioned near the southern extent of the diffuse X-ray source (see Fig. 4 [Pl. 21]). These filaments have a relatively high surface brightness and are actually visible in the POSS and might have been recognized earlier if it were not for the high density of faint stars and H II emission in this area.

Higher resolution optical images were obtained in 1994 June using the Michigan-Dartmouth-MIT (MDM) Observatory 1.3 m McGraw-Hill telescope. The detector used was a 1024 × 1024 Tektronics CCD which gave a 8.′5 × 8.′5 field of view and an image scale 0.″50 $pixel^{-1}$. Three 300 s exposures were taken through Hα (FWHM = 20 Å) and 6450 Å continuum (FWHM = 150 Å) interference filters for each of two adjacent locations in the southern line of filaments. The set of images for each position were bias subtracted, flat-field corrected, and then aligned. The 6450 Å continuum image was then scaled and subtracted from the Hα image, with background and peak levels adjusted or substituted with constants so as to remove or mask the dense star field component. This procedure enhances the visibility of the emission-line filaments in dense star fields like that found for RX J1819.5−1800. A montage of the two processed images covering the eastern and central portions of the southern line of filaments is shown in Figure 5 (Plate 22).

A low-dispersion spectrum of one portion of the filaments was also obtained in 1994 June using the MDM 1.3 m telescope and the Mark III spectrograph. A 600 lines mm^{-1} grism was employed with a 1.″55 × 2′ slit which covered 4700–7100 Å at a resolution of 6 Å. The slit was orientated N-S and positioned near the western end of the remnant's line of NE-SW running filaments (α[2000] = $18^h19^m16^s$, δ[2000] = −18°20.′8). Three 600 s exposures were taken and reduced using IRAF, Hg-Ne comparison-lamp measurements, and standard star observations (Feige 34, HZ 44, BD 25 3941, and BD 40 4032). Sky subtraction was made using slit positions immediately north and south of the filament. Residual [O I] 5577 night sky emission was removed manually from the reduced spectrum using IRAF software. The resulting spectrum is shown in Figure 6.

2.3. CO *Emission from Absorbing Material*

In order to determine the distribution of molecular gas and dust in the direction of G13.3−1.3, we used the 1.2 m millimeter-wave telescope at the Harvard-Smithsonian Center for Astrophysics (CfA) to map a region of ~4 square degrees in the lowest rotational transition of carbon monoxide (CO), the most reliable and widely used tracer of interstellar molecular hydrogen. The CfA telescope is equipped with an extremely sensitive SIS receiver (65 K SSB) and two 256 channel filterbank spectrometers with velocity resolutions of 0.65 and 1.3 km s^{-1} at 115 GHz, the frequency of the CO line observed. The two spectrometers were run simultaneously, the wider one being used primarily to provide emission-free channels for baseline subtraction. Within the region shown in Figure 8 below, spectra were obtained every 10′ (slightly larger than the 8.′7 beam of the telescope) with an rms sensitivity of 0.18 K at $\Delta v = 1.3$ km s^{-1}.

As Figure 7 shows, the CO emission within 1° of G13.3−1.3 is mainly confined in velocity to two broad lanes centered near 20 and 45 km s^{-1}. Spatial maps of the CO emission in these two lanes are shown in Figure 8, with contours of X-ray emission overlaid. Since little emission was detected outside the range 0–65 km s^{-1}, Figures 8*a* and 8*b* together represent

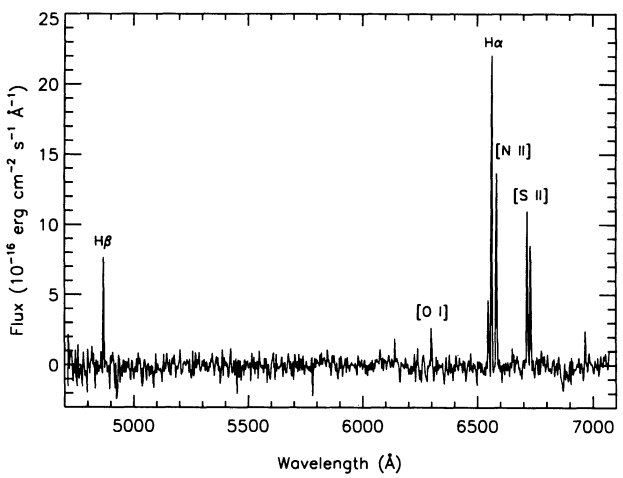

FIG. 6.—Optical spectrum of G13.3−1.3 filaments

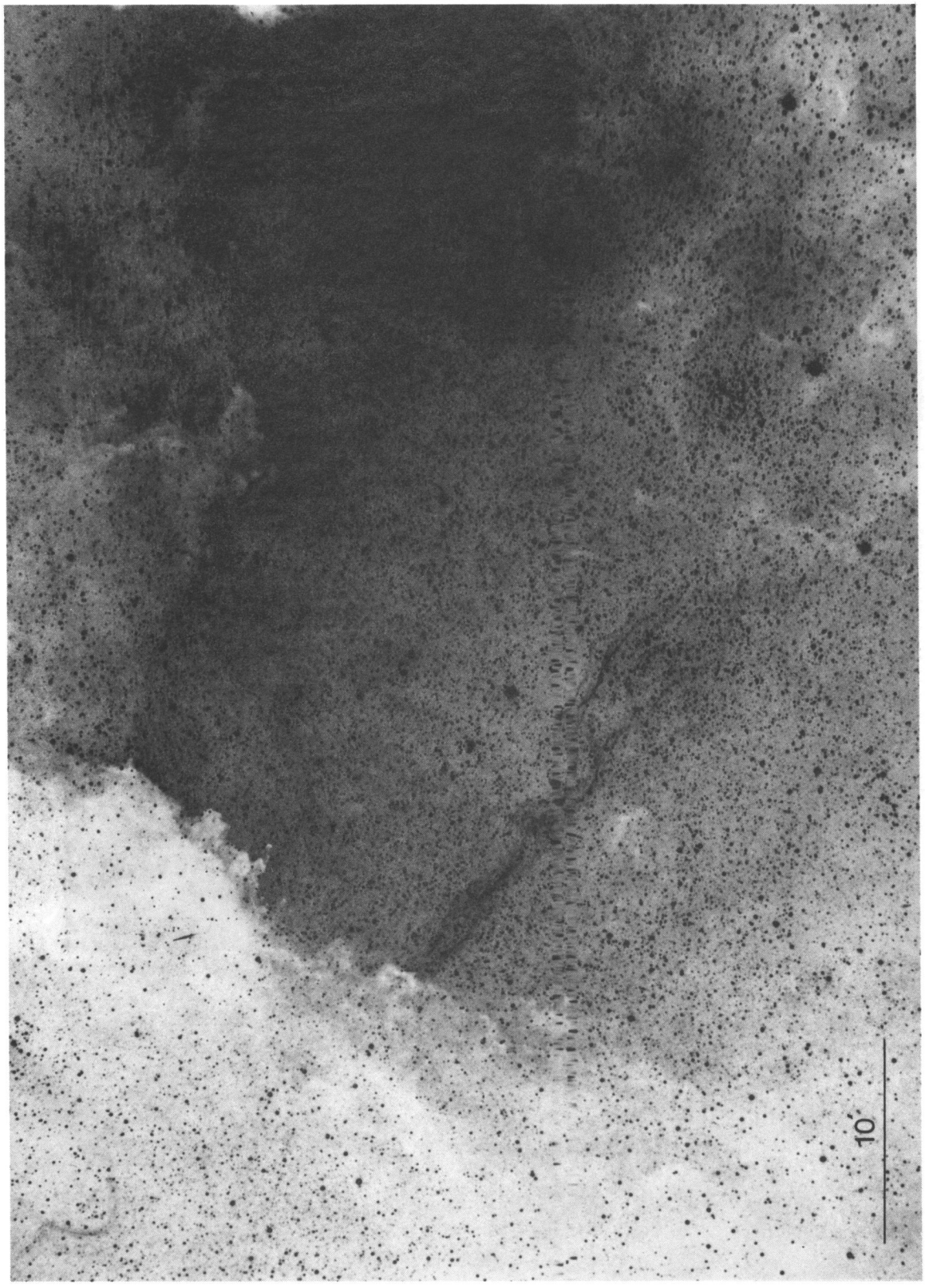

FIG. 3.—Schmidt Hα image of the RX J1819.5−1800 region. In the east lie the dark nebulae Lynds 332, 336, and 342. The H II region, LBN 51, in the west, is overexposed. Note the NE-SW array of filaments just below center and the short, faint filament in the upper left (NE) corner.

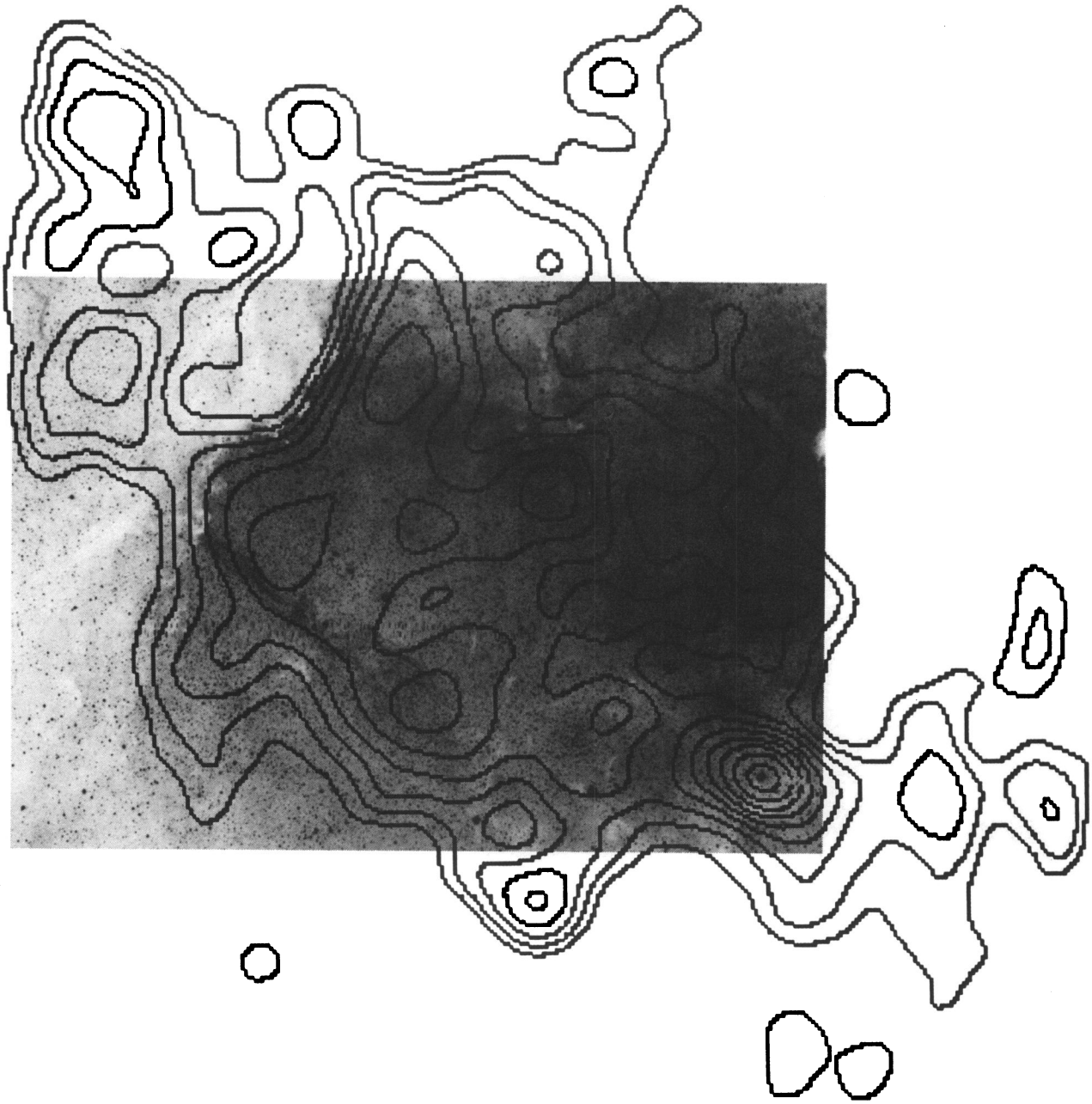

FIG. 4.—Contours of constant X-ray surface brightness overlaid on the Hα photograph of Fig. 3. The SE limb of the remnant is defined by the optical filaments and diffuse X-rays. The region of strong optical extinction coincides exactly with the X-ray gap. In the upper left corner, a section of a contour has been deleted to expose an underlying faint wisp of optical emission.

SEWARD et al. (see 449, 684)

PLATE 22

FIG. 5.—Hα image of the delicate and complex network of optical filaments associated with the diffuse X-ray source G13.3 – 1.3 (RX J1819.5 – 1800)

SEWARD et al. (see 449, 684)

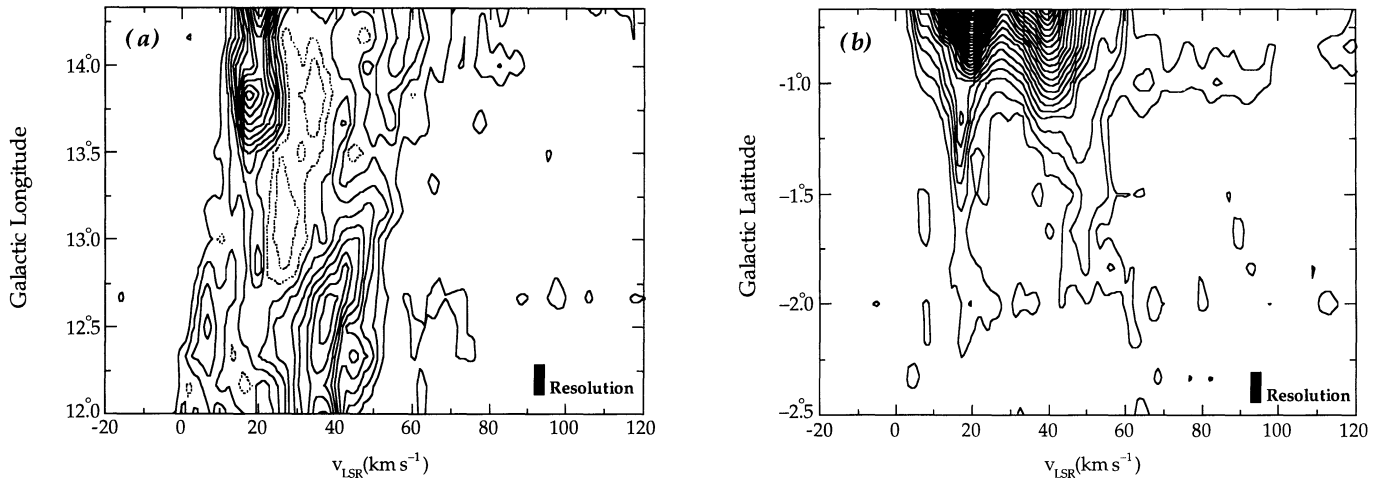

FIG. 7.—(*a*) Longitude-velocity map of CO emission toward G13.3−1.3, integrated from −2°.5 to −0°.5 in Galactic latitude; the lowest contour and contour interval are both 0.22 K deg. (*b*) Latitude-velocity map of CO emission toward G13.3−1.3, integrated from 12° to 14° in Galactic longitude; the lowest contour and contour interval are both 0.18 K deg. In both (*a*) and (*b*) the emission has been smoothed in velocity to a resolution of 2.5 km s^{-1} and the lowest contour is at approximately the 3 σ noise level.

nearly all of the molecular gas detected by our survey. Little CO emission is seen in either map toward the brightest part of G13.3−1.3, confirming that this object lies in a Galactic window of low extinction.

3. DISCUSSION

3.1. *Identification of RX J1819.5−1800 as a probable SNR*

One possible explanation for the nature of the diffuse X-ray source is that the X-rays originate in an O-star association, a situation similar to that of the Carina Nebula (Seward & Chlebowski 1982). The X-rays might then be shinning through a hole between obscuring clouds to form RX J1819.5−1800. However, Humphries (1978) does not list an O-star association in this region and HD 167771 is the only bright O star in the field. Detected X-rays do come from this and another early star but neither is within the region of the diffuse X-ray emission.

Extended galactic X-ray emission also suggests the possibility of a previously unrecognized supernova remnant. The X-ray and optical properties of the source are consistent with a SNR identification though it lacks a recognized nonthermal radio source at this position (Green 1991). The coincidence of the southern X-ray emission ridge with sharp optical filaments, which have an optical spectrum characteristic of shock-heated gas, provides strong evidence for a SNR identification.

The wide-field Schmidt images indicate that the entire line of sharp southern filaments together with the shorter and much fainter NE filaments have unusually strong [S II] $\lambda\lambda$6716, 6731 line emission relative to Hα for ordinary H II region emission. The [S II]/Hα ratio is usually a good indicator of shock-heated gas and the measured value of 0.85 is well within the range seen for Galactic SNRs (Blair, Kirshner, & Chevalier 1981; Smith et al. 1993). The presence of strong [O I] $\lambda\lambda$6300, 6364 emission ([O I]/Hβ = 0.5) is also consistent with a SNR identification (Fesen, Blair, & Kirshner 1985). The lack of detectable [O III] 5007 emission suggests a shock velocity of 60 km s^{-1} or less based on shock emission model comparisons (e.g., Dopita et al. 1984; Cox & Raymond 1985; Hartigan, Raymond, & Hartmann 1987).

If the X-rays originate from shock heating, a temperature of 3.5×10^6 K (0.3 keV) implies a shock velocity of 500 km s^{-1}. Probably the X-ray and optical emission do not originate in the same volume of space, even if both are associated with the rim of the remnant. The X-rays are very faint and it is difficult to derive characteristics accurately; however, the temperature must clearly be higher than 5×10^4 K, which is equivalent to 60 km s^{-1}.

Establishing a firm SNR identification for G13.3−1.3 will require radio observations showing evidence of nonthermal emission. While no obvious source can be seen in the 408 MHz maps of the Galactic plane by Green (1974) and Haslam et al. (1982), in the 2695 MHz maps by Reich et al. (1990) there is a weak ridge of radio emission which coincides nicely with the southern and NE optical filaments detected. The coincidence of radio, optical, and X-ray emission move us to conclude that this is probably a previously unknown SNR. We propose the name, G13.1−1.3, based on the coordinates of the center of the ellipse in Figure 2. Like the earlier *ROSAT* SNR discovery, the radio surface brightness is faint (as is the X-ray surface brightness).

G13.3−1.3's complete structure and size are difficult to determine based on the *ROSAT* PSPC image alone. Whereas to the south, the object is well delineated by the optical filaments, to the NE the X-rays are obscured by a dark cloud. Two patches of X-ray emission and a faint filament visible in the upper left corner of Figures 3 and 4 allow us to trace the edge along the ellipse shown in Figure 2. The NW edge is not obvious in optical data and we have assumed the diffuse X-rays show its position.

It is possible that the remnant could extend further to the NW and is presently invisible behind absorbing material. We may be seeing the southern rim of a larger structure perhaps 1°.5–2° in diameter. A detailed radio map might lead to better definition of the northern part of the remnant.

If the remnant does extend farther to the N, the X-rays in the SE might then come from the rim and those in the NW from the interior. A mixture of shell and interior emission is not uncommon. W28, IC 443, and MSH 15−56 are other rem-

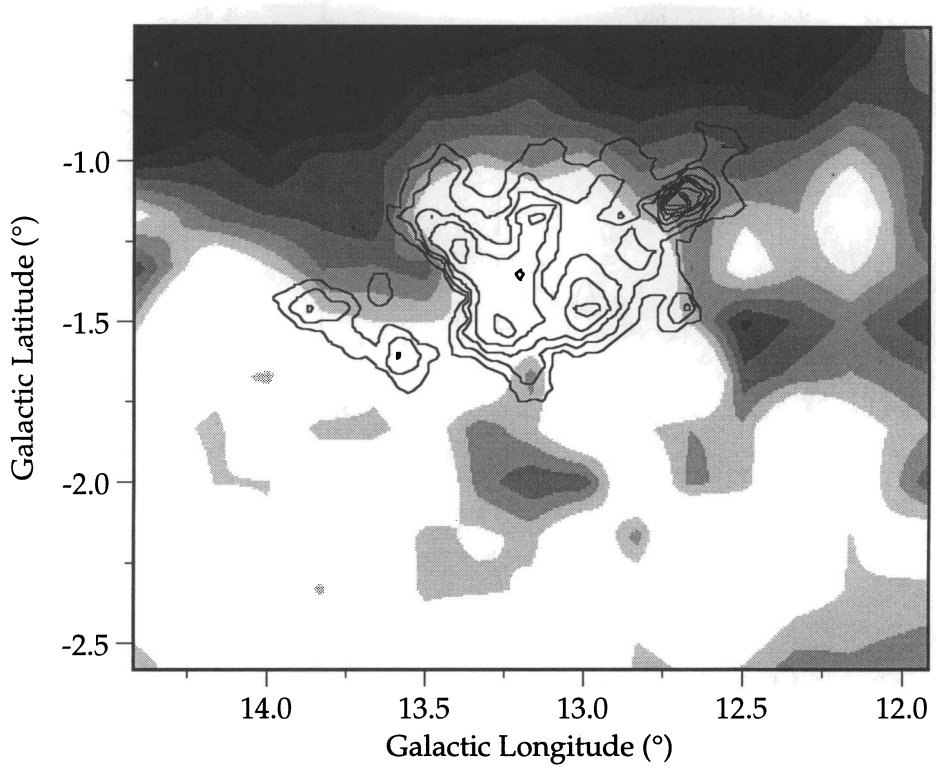

FIG. 8*a*

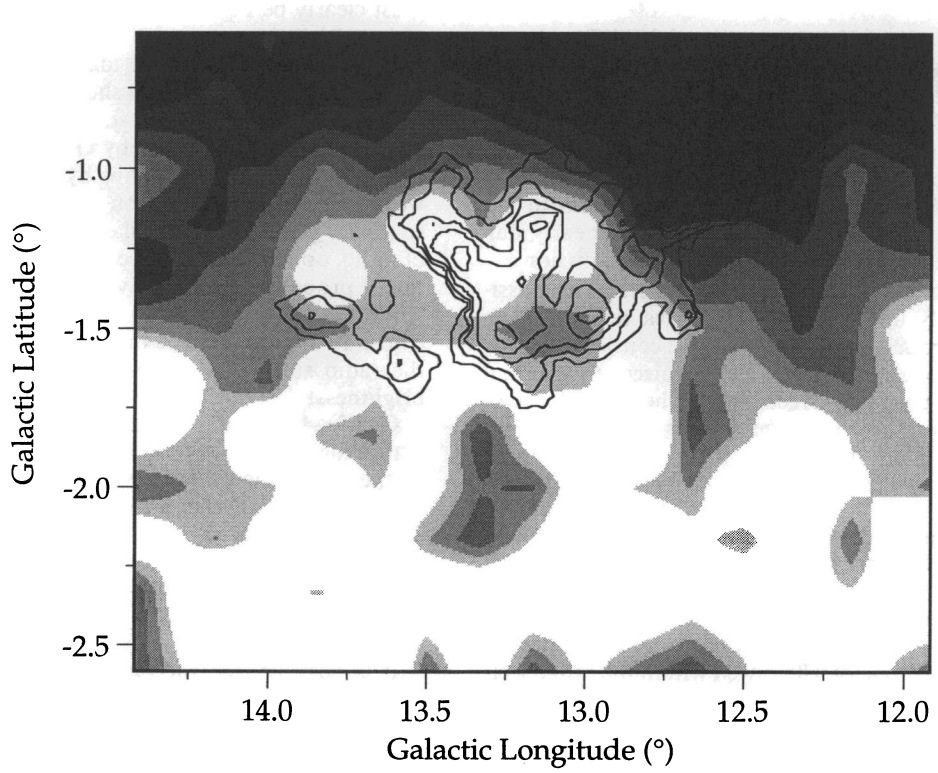

FIG. 8*b*

FIG. 8.—Contours of X-ray surface brightness overlaid on gray-scale maps of CO emission integrated from 0 to 27 km s^{-1} (*a*) and 27 to 65 km s^{-1} (*b*). The CO gray-scale levels are logarithmically spaced a factor 1.5 apart, starting at 2.67 K km s^{-1} in (*a*) and 3.36 K km s^{-1} in (*b*); these are approximately the 2.6 σ noise levels for each. Using a CO-to-H_2 conversion factor of 2.3×10^{20} cm^{-2} K^{-1} km^{-1} s (Strong et al. 1988) and the gas-to-extinction ratio of Bohlin et al. (1978), the lowest gray-scale contours in (*a*) and (*b*) correspond to visual extinctions of 0.64 and 0.81 mag, respectively. The X-ray contours are spaced linearly at 0.0013 count $arcmin^{-2}$ s^{-1}.

nants having X-ray emission both from part of the shell and from the interior (Seward 1990). The unresolved source close to the center might indicate a Crab-like structure but is not strong enough to search for pulsations. We can estimate (Seward & Wang 1988) an upper limit on the rate of loss of rotational energy from any central pulsar. We assume that all the central luminosity is synchrotron radiation and, at a distance of 3.3 kpc, the rate of rotational energy loss is $\leq 7 \times 10^{36}$ ergs s^{-1}, or $\leq 1/70$ that of the Crab Pulsar.

3.2. *Distance and Luminosity*

The proposed SNR lies coincident with the rich starcloud M24 (Burnham 1978) containing the open star cluster NGC 6603 and situated in a galactic "window" between prominent dust clouds. NGC 6603 is 5′ in diameter and is located about 20′ SW of the center of G13.3−1.3 and about 14′ E of the O star HD 167771. Although the cluster lies within the region of detected diffuse X-ray emission, there is no X-ray emission maximum which might be attributed to NGC 6603. Bica, Ortolani, & Barbuy (1993) and Santos & Bica (1993) find a foreground reddening of $E(B-V) = 0.50$ to NGC 6603 and $E(B-V) = 0.60$ for field stars N of the cluster. They assign distances of 3.6 and 4.2 kpc, respectively.

G13.3−1.3 clearly lies behind the absorbing clouds LDN 332, 336, and 342 (Lynds 1962) to the east. Both the X-rays and optical filaments indicate strong attenuation in this region. Yet, the measured $H\alpha/H\beta = 3.5$ along the western end of the optical filaments indicates little reddening with $E(B-V) = 0.15$. This is surprising in view of the considerable dust lanes in the region and is much less than the $E(B-V) = 0.50$ reported for NGC 6603 only 15′ to the SW. However, NGC 6603 is surrounded by numerous small dust lanes (Fig. 3) whereas the optical filaments for which spectra were obtained lie in a rich star field area with no obvious dust clouds present.

The absorbing dust clouds to the east of G13.3−1.3 are clearly seen in the map of CO in the range 0–27 km s^{-1} (Fig. 8*a*) as a "finger" of emission extending down from the Galactic plane to a position near $l = 13.^{\circ}5$, $b = -1.^{\circ}5$. Absorption by this finger of molecular gas almost certainly causes the sharp cutoff of X-ray emission seen on its high-longitude side; the weaker X-ray emission on the finger's opposite side (near $l = 13.^{\circ}75$, $b = -1.^{\circ}5$) may mark the true eastern edge of remnant. At a velocity of 17.6 km s^{-1}, the finger has a near kinematic distance of 2.0 kpc according to the Galactic rotation curve of Clemens (1985). At this low Galactic longitude, the dominant source of uncertainty on the kinematic distance is not the object's velocity or the form of the rotation curve, but the cloud-cloud velocity dispersion of molecular clouds, which is of order 4.2 km s^{-1} (Combes 1991). This dispersion translates into an uncertainty on the near kinematic distance of 0.4 kpc. Thus we adopt 2.0 ± 0.4 kpc as a lower limit for the distance to G13.3−1.3.

An upper limit to the distance is suggested by the CO cloud near $l = 13.^{\circ}2$, $b = -1.^{\circ}5$ in Figure 8*b*, which has a molecular column density comparable to that of the finger, yet does not appear to be absorbing X rays. The lack of absorption suggests that this cloud, with a velocity of 52 km s^{-1} and a near kinematic distance of 4.7 ± 0.4 kpc, lies beyond G13.3−1.3.

The X-ray-measured column ranges from 1.0×10^{21} to 1.0×10^{22}. Starke et al. (1985) give the average total column in this direction as 1.1×10^{22} so the maximum X-ray measured column corresponds to a location beyond the absorbing galactic gas. We assume the X-ray measured column is consistant with the optically derived value, using the average relationship between extinction and H column density of 5.8×10^{21} atoms cm^{-2} $magnitude^{-1}$ (Bohlin et al. 1978). Thus the minimum X-ray column possible is equivalent to $E(B-V) = 0.17$, nearly that measured for the optical filaments. In any case, the relatively small reddening found for the optical filaments is unlikely to be representative of the whole remnant, especially in areas near the dark clouds LDN 332 and 336 and the faint NE filaments.

The reddening of the filaments is $\frac{1}{4}$ that of the field stars in M24 (Santos & Bica 1993), which suggests a minimum distance of 1 kpc. The CO observations show that the distance is between 2.0 and 4.7 kpc. We therefore adopt a distance of 3.3 ± 1.3 kpc.

At this distance, G13.3−1.3 has dimension of $38 \pm 15 \times 67 \pm 26$ pc and the X-ray luminosity, L_x, is $3 \pm 2 \times 10^{34}$ ergs s^{-1}. This is low for an SNR (L_X of the Cygnus Loop is $\approx 10^{36}$ ergs s^{-1}). Of course, if the remnant extends farther to the NW, only part of the X-ray emission is visible and the corresponding luminosity would be considerably larger. Nevertheless, the X-ray discovery of this probable new SNR suggests that still more extended galactic SNR await optical and radio detection.

We thank W. Shoening for assistance using the Burrell Schmidt and R. Downes, D. Wallace and the MDM Observatory staff for help in obtaining and reducing the optical images and spectra. R. A. F's research was funded in part by a Walter Burke Research Grant. F. D. S. was supported by NASA contract NAS 8-39073.

REFERENCES

Aschenbach, B. 1993, Adv. Space Res., 13, 45
Bica, E., Ortolani, S., & Barbuy, B. 1993, A&A, 270, 117
Blair, W., Kirshner, R., & Chevalier, R. 1981, ApJ, 247, 879
Bohlin, R., Savage, B., & Drake, J. 1978, ApJ, 224, 132
Burnham, R., Jr. 1978, Burnham's Celestial Handbook (New York: Dover)
Clemens, D. 1985, ApJ, 295, 422
Combes, F. 1991, ARA&A, 29, 195
Cox, D., & Raymond, J. 1985, ApJ, 298, 651
Dopita, M. A., et al. 1984, ApJ, 276, 653
Fesen, R., Blair, W., & Kirshner, R. 1985, ApJ, 292, 29
Gieren, W. P., & Fouque, P. 1993, AJ, 106, 734
Green, A. J. 1974, A&AS, 18, 267
Green, D. A. 1991, PASP, 103, 209
Gregory, P. C., & Fahlman, G. G. 1980, Nature, 287, 805
Haslam, C. G. T., Salter, C. J., Stoffel, H., & Wilson, W. E. 1982, A&AS, 47, 1
Hartigan, P., Raymond, J., & Hartmann, L. 1987, ApJ, 316, 323
Helfand, D. J., Velusamy, T., Becker, R. H., & Lickman, F. J. 1989, ApJ, 341, 151
Hughes, V. A., Harten, R. H., & van den Bergh, S. 1981, ApJ, 246, L127
Hughes, J. P., et al. 1995, in New Horizons of X-ray Astronomy—First Results from *ASCA*, in press
Humphries, R. 1978, ApJS, 38, 309
Lynds, B. T. 1962, ApJS, 7, 1
——. 1965, ApJS, 12, 163
Pfeffermann, E., Aschenbach, B., & Predehl, P. 1991, A&A, 246, L28
Reich, W., Fürst, E., & Arnal, E. M. 1992, A&A, 256, 214
Reich, W., Fürst, E., Reich, P., & Reif, K. 1990, A&AS, 85, 633
Santos, J. F. C., & Bica, E. 1993, MNRAS, 260, 915
Seward, F. D. 1990, ApJS, 73, 781
Seward, F. D., & Chlebowski, T. 1982, ApJ, 256, 530
Seward, F. D., & Wang, Z. R. 1988, ApJ, 332, 199
Smith, R. C., Kirshner, R. P., Blair, W. P., Long, K. S., & Winkler, F. P. 1993, ApJ, 407, 564
Starke, A., Gammie, C., Bally, J., Linke, R., & Heiles, C. 1985, private communication
Strong, A. W., et al. 1988, A&A, 207, 1
Taylor, J. H., Manchester, R. N., & Lyne, A. G. 1993, ApJS, 88, 529